# TRACE ELEMENT ANALYSIS OF POWDERED BEVERAGES AND OTHER MATERIALS BY X-RAY FLOURESCENCE

by

CHERYL K. DELLAI

B. S., University of Wyoming, 1974

---

A MASTER'S THESIS

submitted in partial fulfillment of the

requirements for the degree

MASTER OF SCIENCE

Department of Physics

KANSAS STATE UNIVERSITY
Manhattan, Kansas

1976

Approved by:

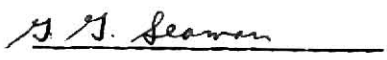

Major Professor

THIS BOOK
CONTAINS
NUMEROUS PAGES
WITH THE ORIGINAL
PRINTING BEING
SKEWED
DIFFERENTLY FROM
THE TOP OF THE
PAGE TO THE
BOTTOM.

THIS IS AS RECEIVED
FROM THE
CUSTOMER.

# TABLE OF CONTENTS

# ILLEGIBLE DOCUMENT

THE FOLLOWING DOCUMENT(S) IS OF POOR LEGIBILITY IN THE ORIGINAL

THIS IS THE BEST COPY AVAILABLE

# LIST OF FIGURES

# TABLES

# CHAPTER ONE

## INTRODUCTION

For the past several years x-ray fluorescence spectrometry, using a lithium-drifted silicon detector, has been used at Kansas State University and other universities to determine the kinds and the amounts of trace elements in various substances.[1, 2, 3] The techniques used to stimulate x-ray fluorescence of trace elements were based on proton bombardment or x-ray excitation. In cooperation with the Agricultural Experiment Station at Kansas State University, the technique of x-ray stimulated x-ray fluorescence has been applied to the problem of determining the kinds and amounts of trace elements in powdered or crystal beverals.

The original motivation for this study was to determine the kinds and amounts of trace elements in powdered beverages, especially coffees, as the information was not easily obtainable for a large number of samples using routine chemical procedures. It was further proposed that this method could be used in screening process for moderately toxic elements.

This technique can be used qualitatively to establish the kinds of elements present in many kinds of materials. Some of these

materials are food stuffs, clothes, draperies, papers, inks, soils, metal alloys, rocks, paints, and pottery glazes. The overall spectrum of a sample can sometimes be used to distinguish between similar inks, alloys, soils, and brand products. In some cases the spectrum may be useful in identifying products from different production lines.[4] This is called signature analysis. Quantitatively, this technique can be used to determine the actual amounts of the elements in samples. This thesis discusses the details of x-ray stimulated x-ray fluorescence and the application of it to trace element identification and analysis in powdered beverages and other materials.

# CHAPTER TWO

## X-RAY FLUORESCENCE

The electron energy levels of a given element are unique because these levels are primarily determined by the number of protons in the element's nucleus. Ionization of an inner shell electron will allow an electron from a higher energy level to fall into the shell with the vacancy, releasing a given amount of energy in the process. The energy can be emitted in the form of photons, with wave lengths in the x-ray region of the energy spectrum for elements with atomic number, Z, above 10. These x-rays are termed characteristic x-rays since they are determined by the difference in energy levels of a given element. Thus, these x-ray energies are unique to that element. The energy spectrum of x-rays can be used to identify the elements present.

To produce vacancies in an inner shell of an atom, the exciting source must have an energy larger than the binding energy of an electron in that shell. This source may be x-ray photons from a radioisotope or a transmission tube. Inner shell vacancies can also be produced by a high energy particle beam of alpha particles or protons.[5,6,10] In this case radioisotopes were chosen as the

energy sources since they required no electronics or power, and are relatively inexpensive. The kind of radioisotope selected depended upon its x-ray energy range, its half-life, strength, shielding requirements, and the samples to be analyzed.

In the interaction of photons with matter in the x-ray energy range, three processes are important. These are the photoelectric effect, the elastic scattering of photons, and the compton scattering of photons. The photoelectric effect is the dominant process for removing inner shell electrons from an atom. Elastic scattering does not eject any electrons, while compton scattering is most likely to remove outer shell electrons.

Elastic scattering is a process where the photons of the fluorescing or primary radiation are scattered by electrons that are so tightly bound to an atom that no ionization or excitation is possible. This process is favored for low photon energies and heavier elements.

Compton scattering is inelastic scattering in which the initial photon collides with atomic electrons essentially as if they were free electrons. The photon will lose energy and change direction according to the scattering angle, $\Theta$, as indicated in Equation 1.

$$E' = E_o \left(1 + \frac{E_o}{mc^2} (1 - \cos \Theta)\right)^{-1}$$

where $E'$ = Scattered Energy
$E$ = Incoming Energy
$MC$ = Rest Mass of the Atom

The relative probability for the photoelectric, elastic and inelastic scattering of photons is shown in Figure 1.

X-ray fluorescence is the generation of secondary radiation by an atom after absorbing photons from a primary x-ray sources. To fluoresce in the x-ray region, an atom requires a minimum energy equal to the binding energy of an electron in a given shell. Thus, there are discontinuous photoelectric absorption edges at such critical energies. The maximum photoelectric absorptive cross-section occurs just above the critical binding energy.

The number of x-rays absorbed in or transmitted through a given material can be calculated from the absorption coefficient of the sample, and the path length through the sample. The absorption coefficient, $\mu_m$, is proportional to the matrix density, the cross-section, Avogadro's number, and the atomic weight, summed over all elements. This absorption coefficient can also be represented in terms of the molecular cross-section, the molecular weight, the matrix density and Avogadro's number. Equations 2 and 3 represent each method respectively.

The cross-section used in the absorption calculations to obtain the number of inner shell vacancies that yield fluorescent x-rays should be the photoelectric cross-section. These cross-sections

**THIS BOOK CONTAINS NUMEROUS PAGES WITH DIAGRAMS THAT ARE CROOKED COMPARED TO THE REST OF THE INFORMATION ON THE PAGE.**

**THIS IS AS RECEIVED FROM CUSTOMER.**

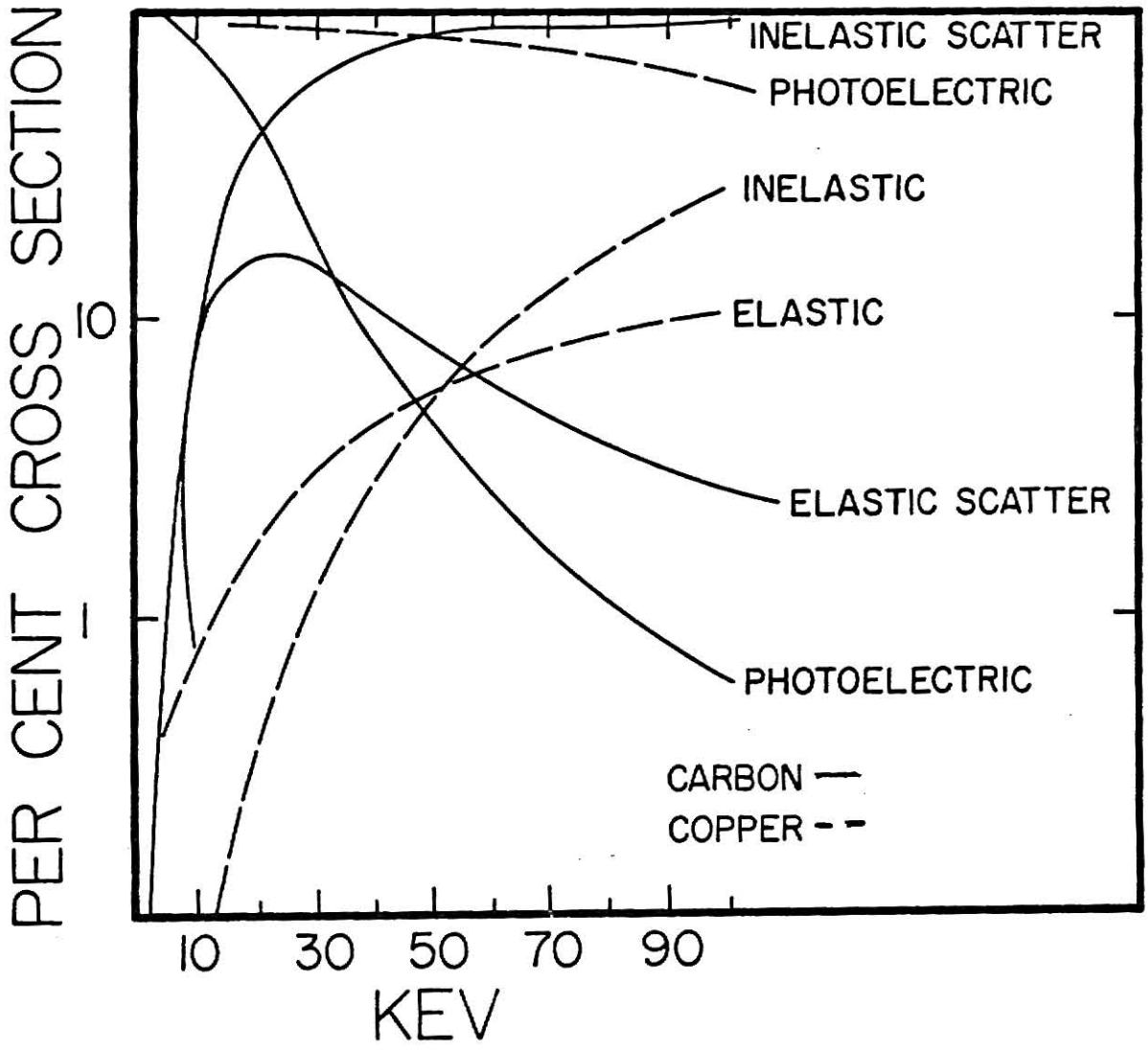


Figure 1. Relative Contribution (total 100%) of Photon Interaction Modes vs Photon Energy for Carbon and Copper

are tabulated for each electron shell.[9] To calculate absorption of x-rays in a material by any process, the total cross-section should be used.

$$\text{Transmission} = \exp - \left(At \sum \frac{f_e \rho_e \sigma_e}{m_e}\right) \qquad (2)$$

$A$ = Avogadro's number
$t$ = thickness of matrix in cm
$\sigma_e$ = cross-section of the element in $cm^2$
$m_e$ = mass of the element in gm
$\rho_e$ = density of the compound in which the element exists in gm/cc
$f_e$ = the fraction of sample due to the element

$$\text{Transmission} = \exp - \left(At \sum \frac{f_i \rho_i \sigma_i}{m_i}\right) \qquad (3)$$

$\rho_i$ = density of the compound in which the element exists in gm/cc
$f_i$ = the fraction of the sample due to a given compound
$m_i$ = molecular weight of a compound
$\sigma_i$ = the cross-section of a compound computed in $cm^2$ as $\sigma_i = \sum \sigma_{ii} f_{ii}$
$\sigma_{ii}$ = the photoelectric cross-section of an element in the matrix
$f_{ii}$ = fraction the compound due to a given element,

The process of excitation consists of an electron absorbing the primary exciting radiation and being ejected from that shell, leaving the resultant ion in an excited state. In the case of a K-electron ejected from an atom, an electron from an outer shell can jump to the free state (N=1) emitting the characteristic K x-rays in the process. The energy of the emitted x-ray will be determined

by the difference in energy of the K-shell and the shell from which the electron jumped to fill the vacancy. The ejection of an electron from the L or M shell would, in a similar manner, lead to the production of the characteristic L & M x-rays. Emission of the K x-rays will be accompanied by higher level emissions.

The Auger effect is competitive with the emission of x-rays. In the low weight elements this effect reduces the K x-ray yield significantly, while increasing the L & M x-ray output. In general, an Auger electron is an atomic electron that receives enough kinetic energy to be ejected when an electron falls to fill a shell. In the case of the K x-rays, a second vacancy is created by the ejection of an Auger electron as if there were secondary internal photoelectric absorption of the K x-rays. The first vacancy was produced by an electron jumping from the L shell to the unfilled K shell as previously described.

It is convenient to account for the Auger effect by defining a ratio of the number of emitted x-rays of a given type to the number of primary vacancies. This ratio is called the fluorescence yield, and is much less than one for the lighter elements, where it is less than 10%, as seen in Figure 2. The calculated fluorescence yield per series per element vary among authorities.[7]

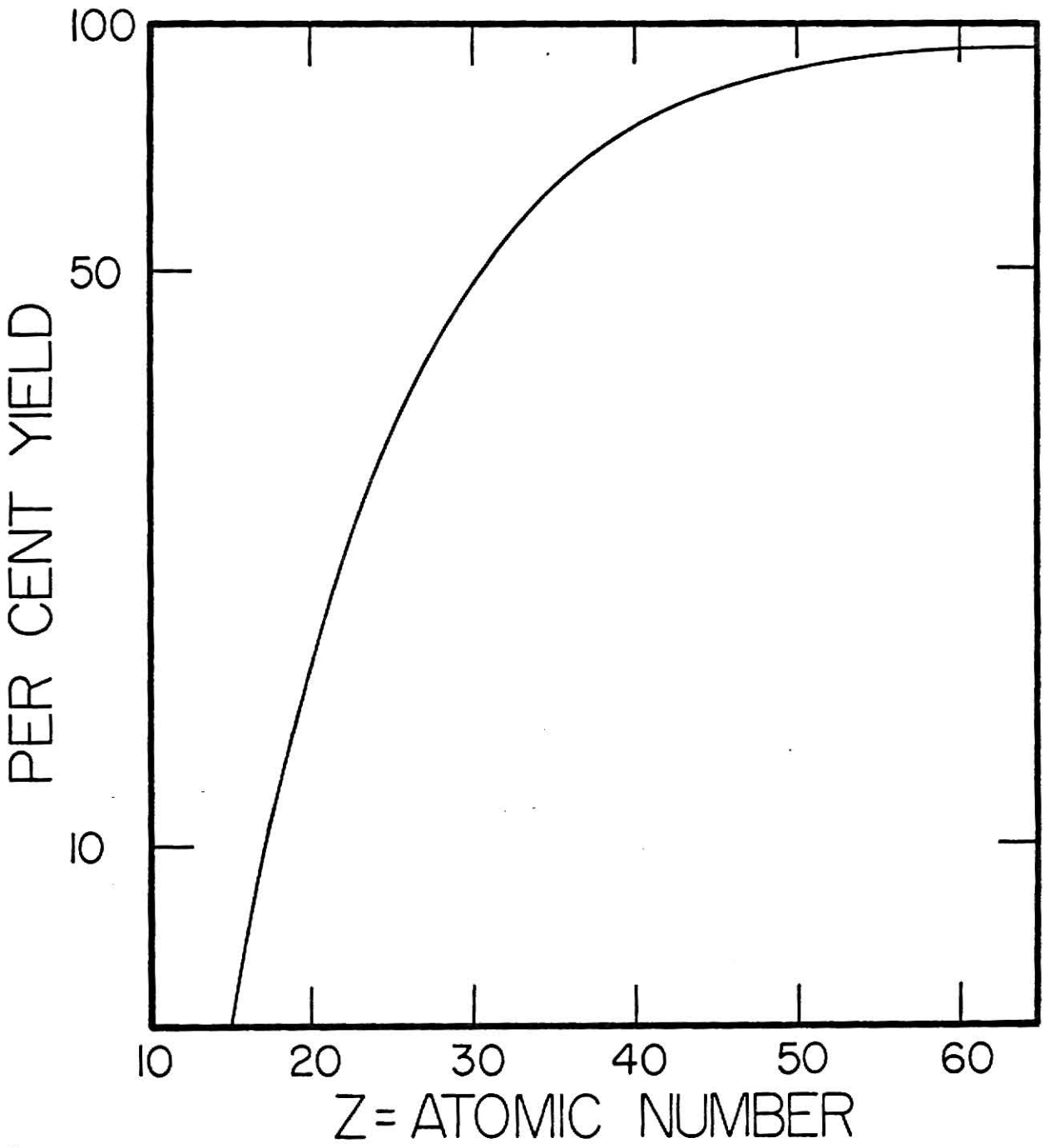


Figure 2. Flourescence Yield ($w_k$) for Elements Z= 15 to 65

Since the energy levels of each element are unique, each element will have a characteristic spectrum which can be used to identify that element. The chemical state of an atom cannot be identified by ionization of the inner shell electrons. The spectrum produced by each element is relatively uncomplicated because the number of electron shells and the subsequent emission lines are few. Sometimes, the peaks of one element may overlap the peaks of another element. Such an overlap can be identifed by the presence or absence of known K or L peaks for the suspected elements. An estimate of the overlap peak size per element can be made and subtracted out. The $K_{\alpha}$ peak of an element is about 10 times greater than the $K_{\beta}$ peak. Characteristic L x-rays from heavier elements will have two peaks of about equal size next to each other and a smaller peak positioned at a higher energy.

# CHAPTER THREE

## DESCRIPTION OF THE SYSTEM

### A. Radioactive Sources and Sample Preparation

The system used to detect trace elements consisted of an excitation source, a sample support system, and a pulse analysis system. Data from the pulse analysis system was analyzed with a PDP-15 computer.

Each source was shaped like a doughnut and was enclosed in shielding material. Each of the sources irradiated the samples directly as seen in Figure 3. Each holder was designed to hold a circular lucite disk 12 mm from the source center. The disk was held in place by a long cylinder taped to the outside. The support system was aligned with the beryllium window on the front of the x-ray detector, and enclosed the window and the detector casing.

In this experiment the x-ray sources were radioisotopes of Fe-55, Cd-109, and Am-241. The Fe-55 source, 25 mCi in strength, decays to Mn-55 by electron capture. The resultant $K_{\alpha}$ and $K_{\beta}$ x-rays of manganese, 5.9 and 6.5 Kev, served as the primary energy source. This source has a yield per disintegration of 26%.

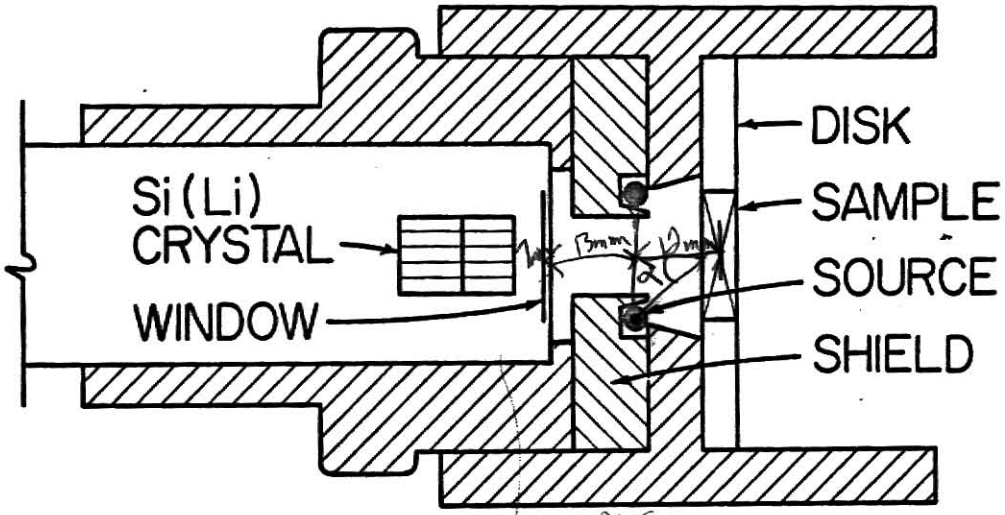


Figure 3. Sample and Source Holder Interlocked with the Detector. The window is made up of beryllium; the casing, aluminum; the shielding, lead; the sources are iron, cadmium, and americium; and the disk is made of lucite.

Its half-life is 2.7 years. This fact was taken into account if the readings were taken more than several months apart. The Cd-109 source, 2 mCi strong, decays to Ag-109 by electron capture. The resultant $K_{\alpha 1,2}$ and $K_{\beta 1,2}$ x-rays, 22 and 25 Kev, served as the primary exciting radiation. The Cd-109 source has a theoretical yield per disintegration of 107%. Its half-life is 453 days. Here again, this fact was taken into account if the readings were taken more than one month apart. The Am-241 source, 10mCi strong, decays to Np-237 by alpha decay. The Am-241 source has a theoretical yield per disintegration of 36% for x-rays. The primary exciting radiation is actually a gamma ray at 59.47 Kev. There is a subsequent backscatter peak at 49 Kev, and x-ray at 26.4 Kev. The x-radiation interferes with tin and antimony K x-rays.

To prepare a sample, a lucite disk with a center hole of 1.5 cm in diameter, 3mm in depth, was used. Each disk weighed between 5.9 gm and 7.6 gm. The samples in the disk were sealed between two strips of scotch tape containing no trace elements. Each sample matrix was a dry solid containing light elements. Each sample was prepared from a newly opened vacuum packed container with the exception of the orchard leaves. No special drying procedures were used for any of the samples with the exception of the orchard leaves, which were prepared according to the NBS bulletin.[25] Both the sample and any doping element were as finely ground as possible, and thoroughly mixed.

A balance was used to weigh a disk with one side sealed. After that, the sample was packed in the disk tightly. The sample in the holder was reweighed to determine sample weight. The sample was then sealed and marked. Five samples from five different containers per product were prepared for the major instant coffee brands, instant tea, Carnation instant milk, and the Koolaid brands.

B. X-Ray Detector

The energy analysis system consisted of a protective window, a solid state detector, a preamplifier, a pulse amplifier, a pile-up rejector, and a pulse height analyzer as seen in Figure 4. The window had a thickness of .025 mm of beryllium with a 200 Å gold layer. The window-to-detector distance was 7 mm. Due to the window thickness the x-rays with energies below silicon were effectively blocked. However, due to the low fluorescence yield of elements below sulfur, the effective limit was 2.3 Kev, the K x-ray of sulfur.

The detector consisted of lithium-drifted silicon Si(Li) with a .1 μm dead layer and a sensitive thickness of 5.3 mm. Its diameter was one cm.[12] The Si(Li) semiconductor's ability to serve as a detector results from its capacity to absorb radiation, emitted or reflected from the sample, and become ionized. Once ionized, the

Figure 4.

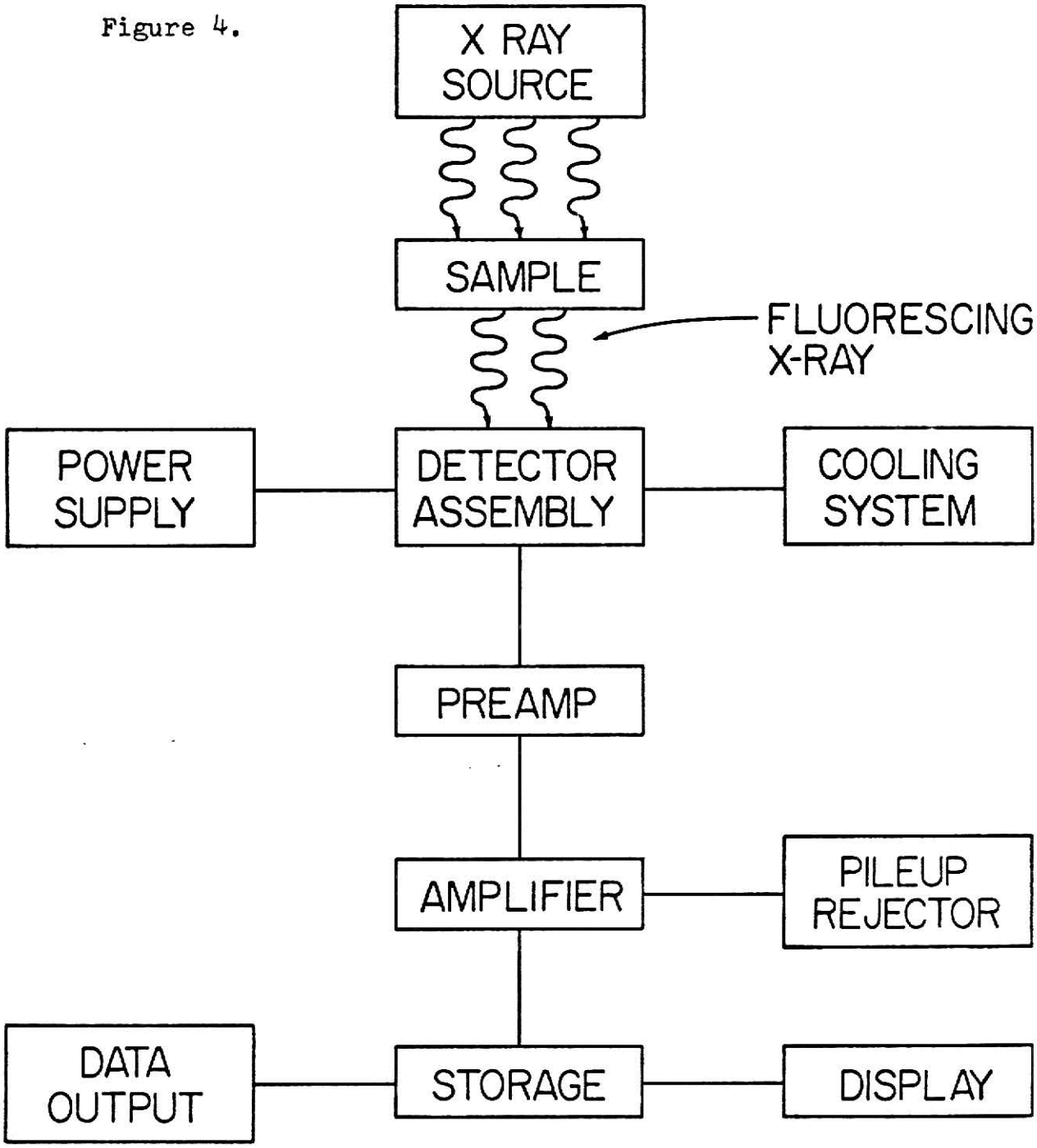


BLOCK DIAGRAM OF APPARATUS

Si (Li) semiconductor becomes conducting. This ionization is termed "the creating of a hole." In the quiescent state, there is a very little current flow. Absorption of a photon creates an amount of "free" charge which is, ideally, proportional to the energy deposited by the incident charge. This charge, the electron-hole pairs, is swept out of the detector by the applied potential as a charge pulse, which in turn forms the basis for qualitative "detection" of the event. This is in addition to carrying a measure of the energy of the absorbed particle. The proportionality between the charge and the deposited energy is the key to x-ray spectrometry.

All of the photon energy deposited on the detector must be converted into electron-hole pairs for good energy response. The resulting large number of electron-hole pairs will define the statistical "size" of the charge pulse. The high resolution capacity of the semiconductor detector rests on the high statistical precision in the photon to charge conversion.

The detector efficiency is virtually 100% between six and twenty Kev, as indicated in Figure 5.[13] On the low energy side the decrease in efficiency is due to absorption in the beryllium window. On the high energy side the detector efficiency decrease is due to the small size of the Si (Li) detector.

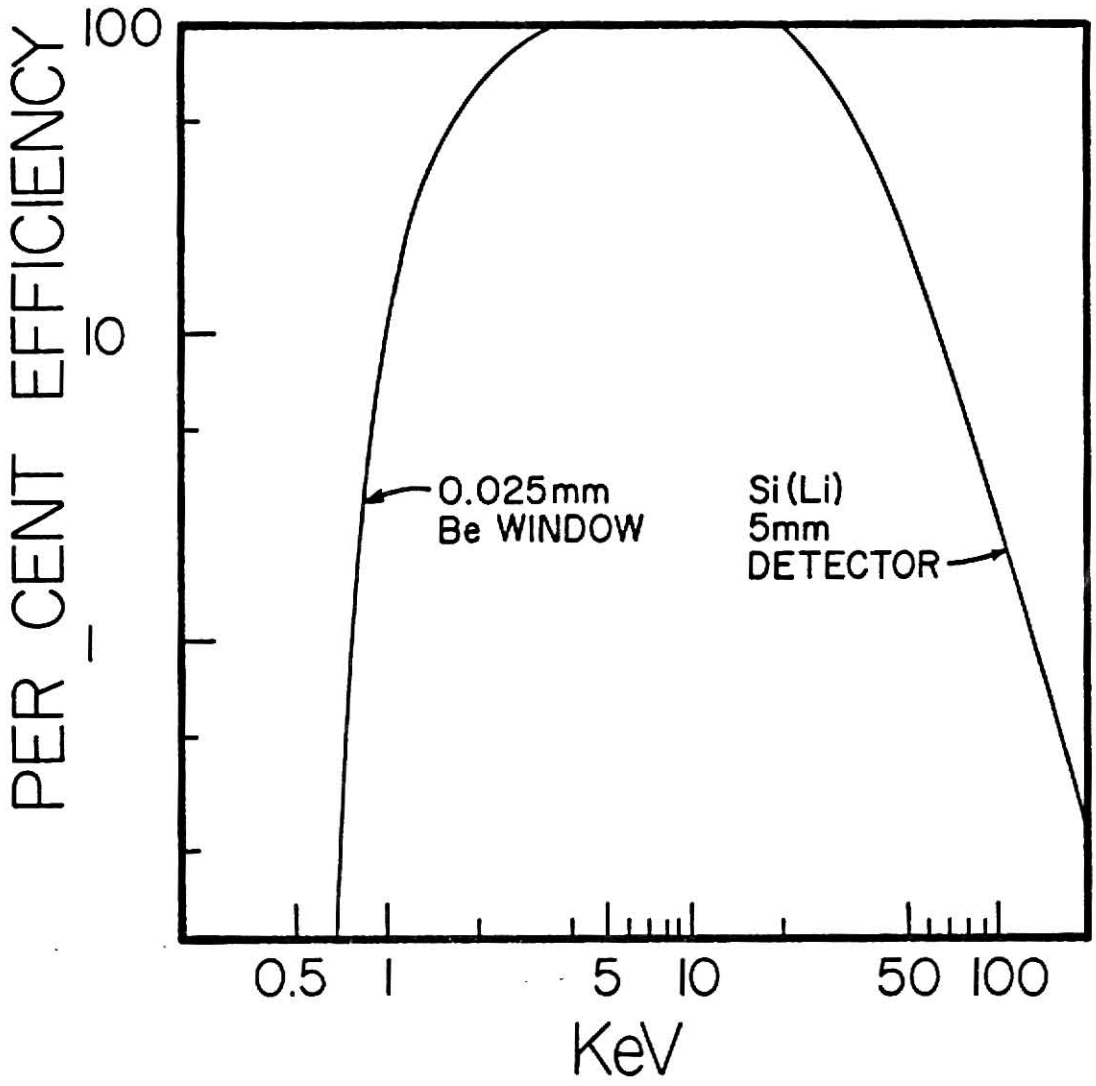


Figure 5. Detector Efficiency as a Function of X-ray Energy

The detector efficiency for the x-rays produced with the Fe-55 source increased from 50% for sulfur to 99% for chromium. The fluorescence yield for the K x-rays varied from 7.62% to 28.2%.[7] Absorption is important for both the primary irradiating source and the fluorescent x-ray. Underlying L & M x-rays from yttrium to uranium can be a problem, but their existence can be determined by locating their K or L series in other spectra. Estimation of the respective L or M peak size is difficult due to the lack of peak separation of the K x-rays for the low atomic numbers and an inability to set a reliable background level. Scotch tape will effectively absorb both sulfur and chlorine K x-rays. Therefore, scotch tape cannot be used except as backing.

The detector efficiency for the x-rays excited with the Cd-109 source was approximately 100% for elements from potassium to ruthenium for the K x-rays.[13] The silver K x-rays were not absorbed by light element samples like carbohydrates. However, the absorption of the secondary radiation was important for those trace elements with atomic numbers below zinc (30). Scotch tape was applied on both ends of the disk. Underlying L x-rays in the middle energy channels were observable and could be subtracted out.

The Am-241 source had no primary absorption problems. The secondary absorption was a problem only on the low-energy end which

overlapped with the Cd-109 source range. Detector efficiency decreased from 100% at yttrium to 55% at neodymium. The fluorescence yield for the K x-rays was virtually 90%. Lead peaks of L x-rays were present in the spectrum due to lead shielding. There was a problem with tin and antimony determination due to the presence of x-rays for the $\alpha$-decay of Am-241 as previously mentioned.[14]

The geometrical factor was determined by the distance between the detector and the sample, their alignment, and the detector area, as seen in Equations 4 and 5.

The geometrical efficiency for each source was approximately 9.6%.[15]

$$\text{Geometrical Efficiency} = \frac{\Omega}{4\pi} \times 100\% \qquad \text{where} \quad \Omega = \int_{\omega_1}^{\omega_2} d\omega \quad (4)$$

$$\text{where} \quad \omega = A\frac{\cos\alpha}{d^2} \quad (5)$$

w = solid angle increment

A = effective detector energy

d = distance between detector and sample

$\alpha$ = angle between the point source and the normal to the detector located at the detector center

C. Electronics and Data Collection

The preamplifier integrates the charge pulse and converts it into a voltage pulse that is proportional to the charge pulse. At this stage noise must be kept low. For counts under 2 x 10 5cts./sec. for 6.4 Kev x-rays, the system is considered linear. The amplifier amplifies the signals and acted as a processor. At this point the baseline is stabilized. Signals will also add onto each other at high counting rates, giving false peaks at higher energies. These pulse pileup distortions are eliminated by a two-signal pileup rejector.[16]

The operation of the linear amplifier with the pileup rejector necessarily imposed a dead time on the system. The "dead time" during which the system can't receive signals, can be corrected for using a live-time clock. With a live-time clock, the actual analysis time per sample is known.[17] Typical dead time levels using a normal counting clock was about 5% to 10% in this experiment.

Following this linear system is a multichannel analyzer (MCA). The multichannel analyzer performs a sorting function on the pulses presented by the linear system and stores them as the counts in the memory of the MCA. The MCA separates counts in energy bins, defined in terms of Kev / channel. This Kev / channel ratio was adjusted for each source to spread the energies over 256 channels.[18]

The data collection began with the adjustment of the system for the source used. The sample disk was placed in the holder. The holding cylinder was inserted and secured. Data from the memory unit was transferred to paper tape, then to magnetic tape. This data was analyzed on a PDP15 computer.

In typical spectra shown in Figures 6 and 7 the three effects of photon excitation are apparent. The continuum at the low energy end of the spectrum and the characteristic drop is caused by compton scattering and the subsequent escape of the scattered photon from the detector as these events are lost from the continuum. It is present whenever mono-energetic or continuum radiation is present. There is an escape peak produced by the silicon in the detector which decreases the incoming parent energy and subsequent detector efficiency. This escape peak is only a .3% - .5% effect at the energies involved.[19] The compton scattering by the detector is most prominent for the Am-241 source where inelastic scattering dominates for such light matrices as food stuffs. At the high energy end are the primary energy peaks. Some of the peaks have been compton scattered due to the irradiated sample, while others have been elastically scattered.

In between are the peaks due to x-ray fluorescence by various elements. The background counts are due to incomplete collection of electrons in the detector as seen in Figures 6 and 7. In samples where

# ILLEGIBLE

# THE FOLLOWING DOCUMENT (S) IS ILLEGIBLE DUE TO THE PRINTING ON THE ORIGINAL BEING CUT OFF

# ILLEGIBLE

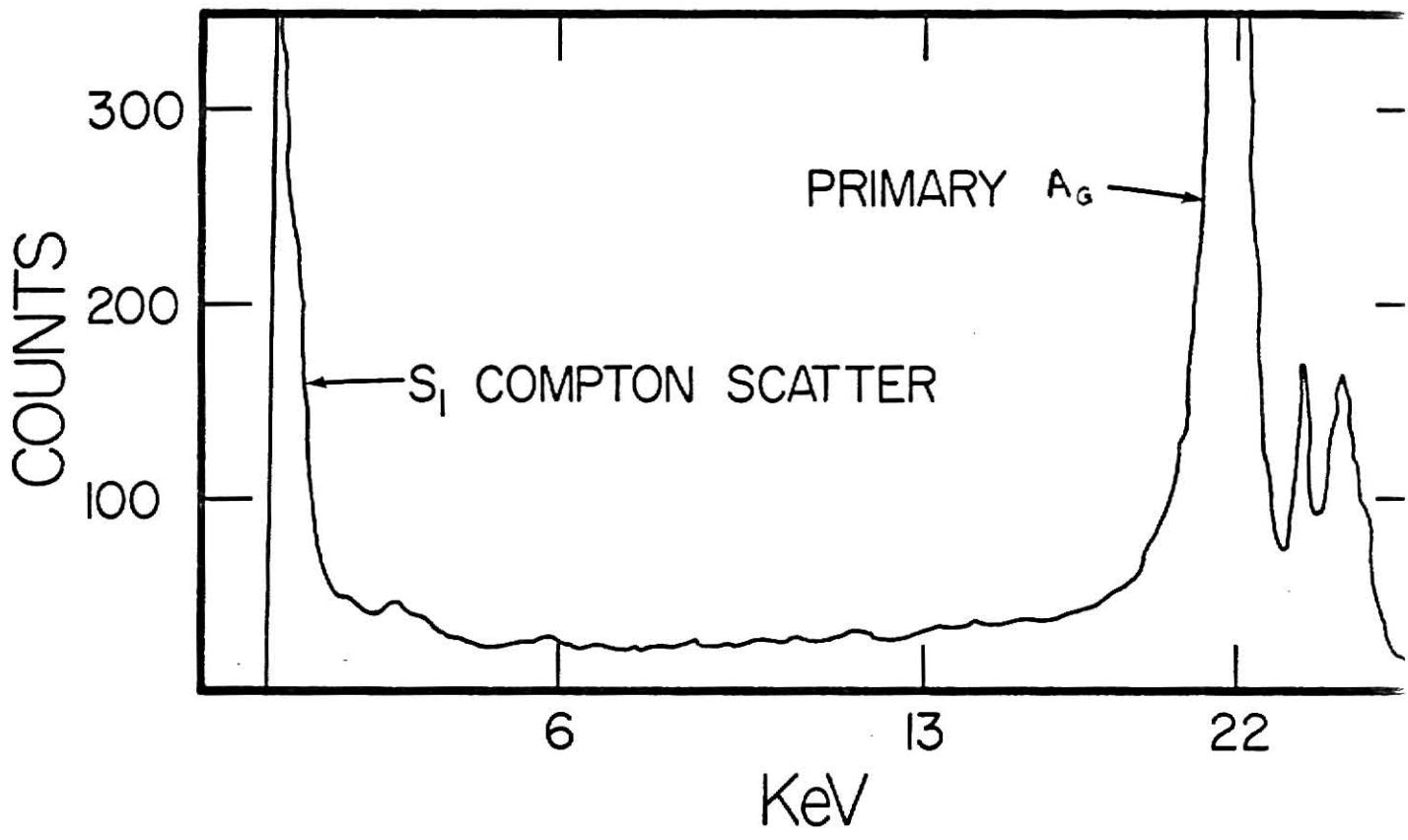


Figure 6. Background Energy Spectrum for Cd-109 Source

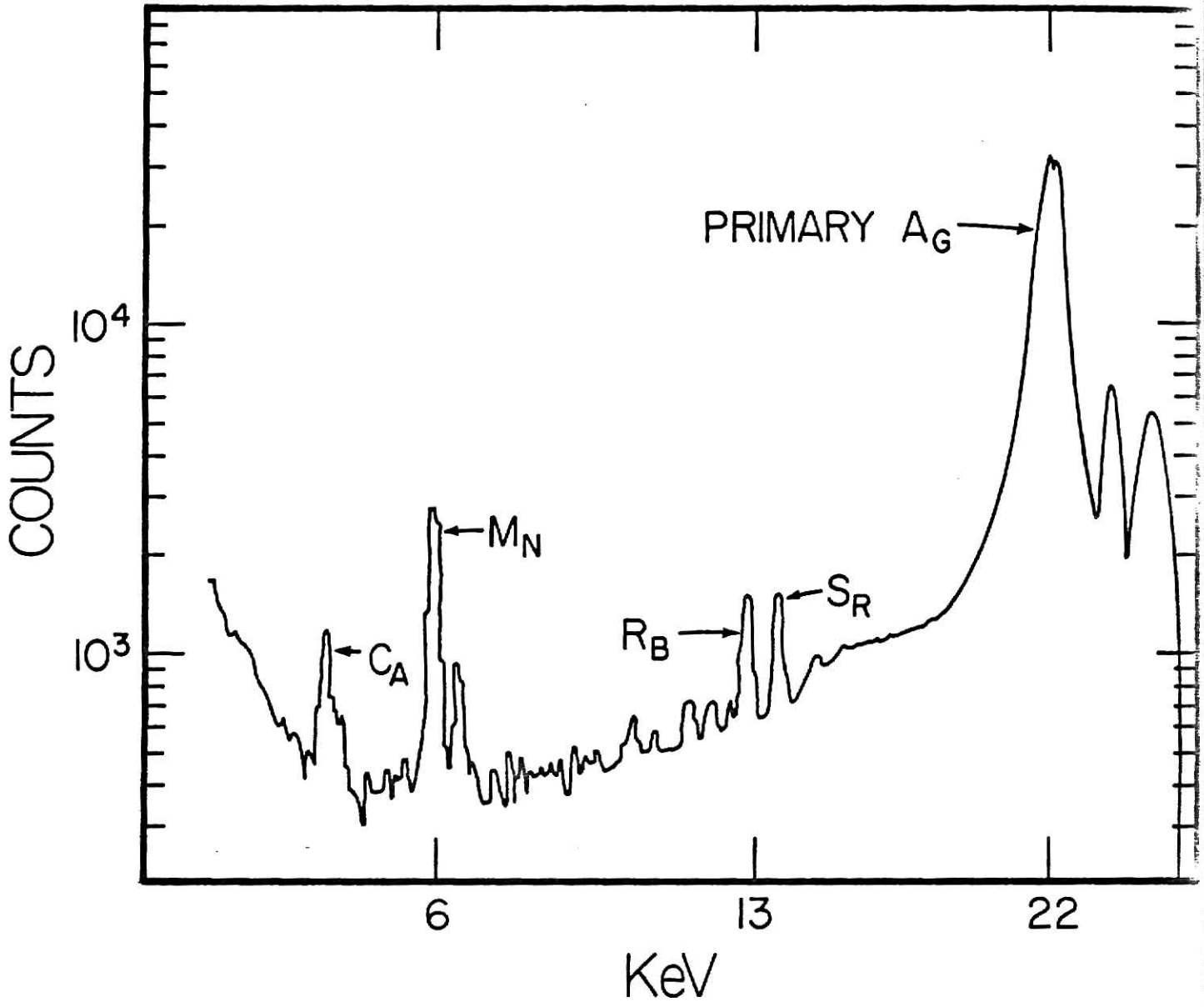


Figure 7. Energy Spectrum of Manganese-Doped Coffee Sample

trace elements were in low concentration, the number of counts in the fluorescent peaks was a small part of the total number of counts. In the high concentration, trace element fluorescent peaks were approximately equal to the number of counts in the scattered and coherent primary x-ray peaks. The scattering produced by the various matrices were useful in determining its relative concentrations. But only the fluorescence peaks for a given matrix were useful in determining the trace element content of a sample.

The live-time per sample was normalized at 3000 seconds for nondoping samples. For doped samples 300 seconds live running time was sufficient. The peak area was then normalized to 3000 seconds so a comparison can be made with the samples. Peak areas were obtained by subtracting from the data a least squares fit to the background. There is usually a 10% error in sample analysis, due to uncertainties in the number of counts in the individual channels, and in the determination of the background.

# CHAPTER FOUR

## CALCULATION OF SYSTEM EFFICIENCY

### A. Calculation of Relative Efficiency

The system's efficiency for the production and the detection of K x-rays depends upon the photoelectric cross-section for producing a K-shell vacancy, the ratio of the $K_\alpha$ x-rays produced to all the K x-rays produced, the fluorescence yield and the detector efficiency.[20]

$$E(K_\alpha) = K E_d(E)\, W_k(Z)\, f(E)\, P_k(K) \qquad (5)$$

$E(K_\alpha)$ = overall efficiency for K peaks

$K$ = constant of geometry due to the detector and sample positions. This is normalized to one for each source

$E_d(E)$ = detector efficiency

$W_k$ = fluorescence yield for the K-series

$f(E)$ = fractional component of $K_\alpha$/K-Total ratio

$P_k(Z)$ = sum of the photoelectric cross section for absorption of the $K_\alpha$ peaks from Fe-55, Cd-109 sources, or the 60 Kev line for the Am-241 source

Self-absorption of the element and absorption by the sample

were not considered here, but were taken into account in computing the experimental curve. These calculated curves are seen in Figures 8, 9, and 10. To compare the experimental curve to the calculated efficiency curve, the heaviest element value was fixed to the corresponding calculated point as in Figure 11.

B. Experimental Calibration Samples

Experimental curves were based on element standards in the sample materials. To make element standards for a given material, the number of doped elements per disk were limited to one. The compound containing the desired element was a non-hydroscopic compound with a low element-weight-to-molecular-weight ratio containing no heavier or nearby lighter weight element than the element desired. The doped compound's weight in the sample was approximately 1% of the total sample weight. These compounds are listed in Table 1. The amount of element in the sample was equal to the compound weight times the ratio of the element-to-molecular weight. The compound and the sample were mixed together by vigorous shaking for at least one minute. These doped samples were prepared at two different concentrations with two to three disks per element per concentration. The test tube weight was first determined, and then the sample was placed in

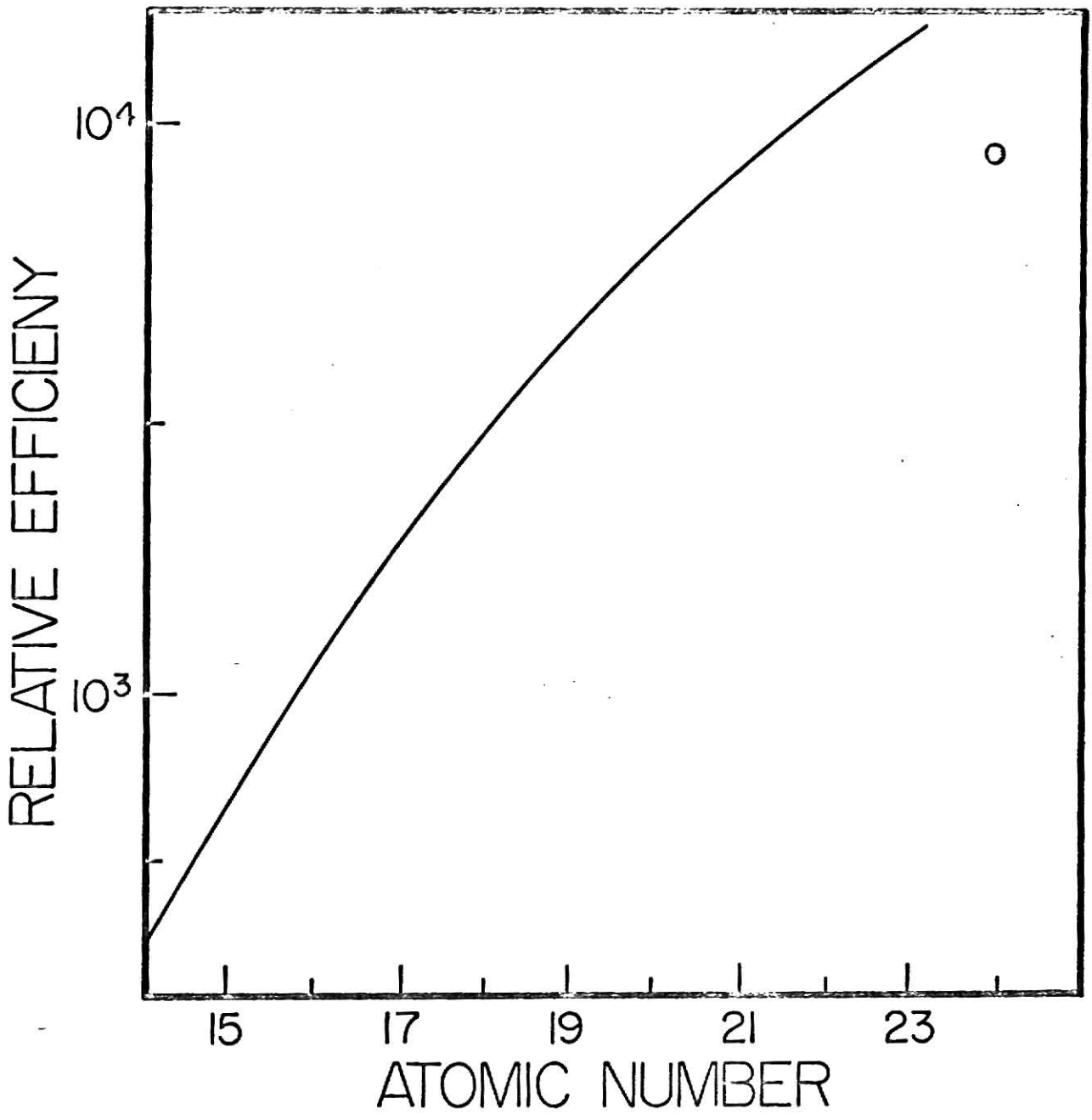


Figure 8. System Efficiency Product Curve For Fe-55 As Calculated by Equation 6

Figure 9. System Efficiency Curve For Cd-109 As Calculated By Equation 6

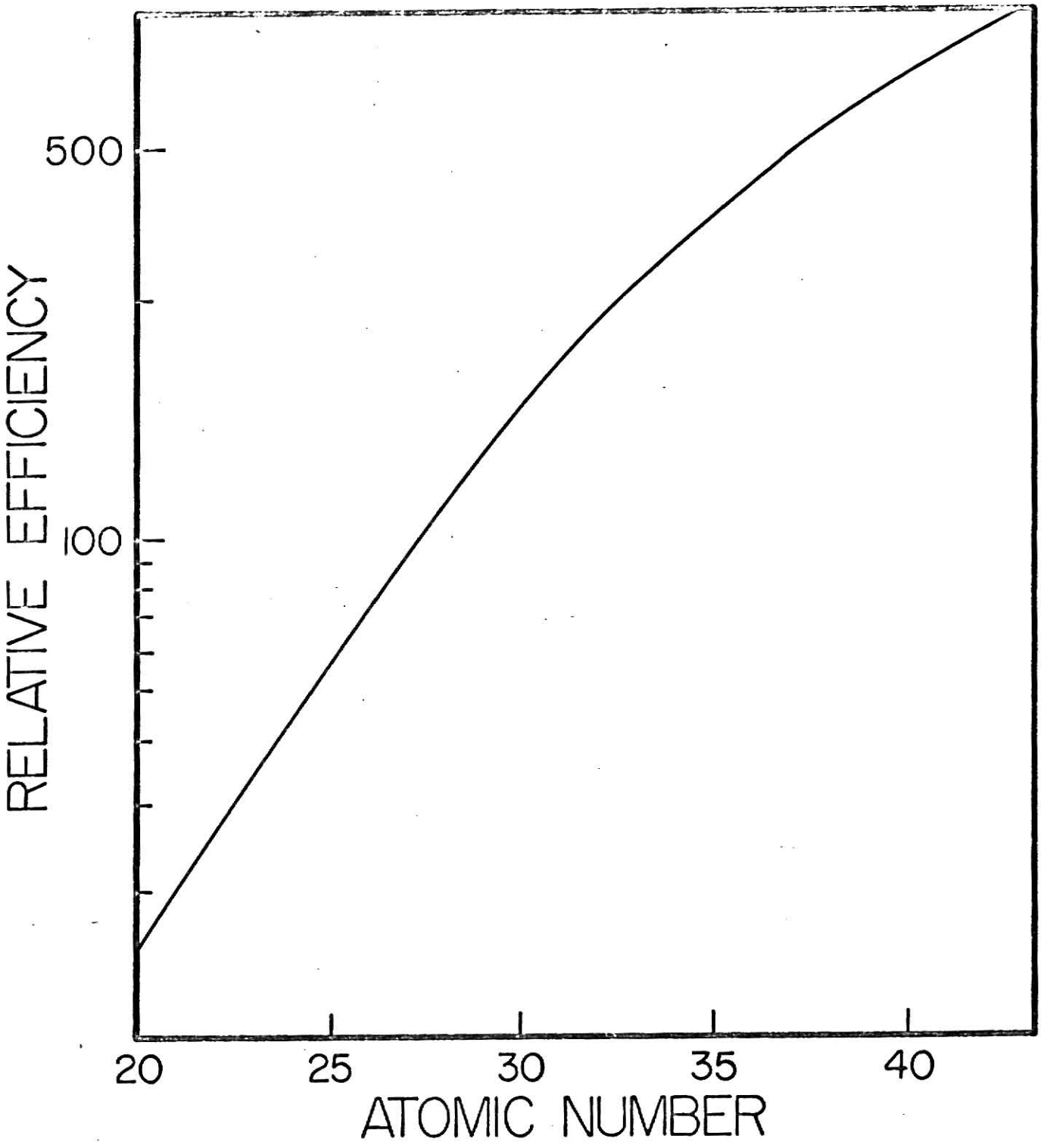

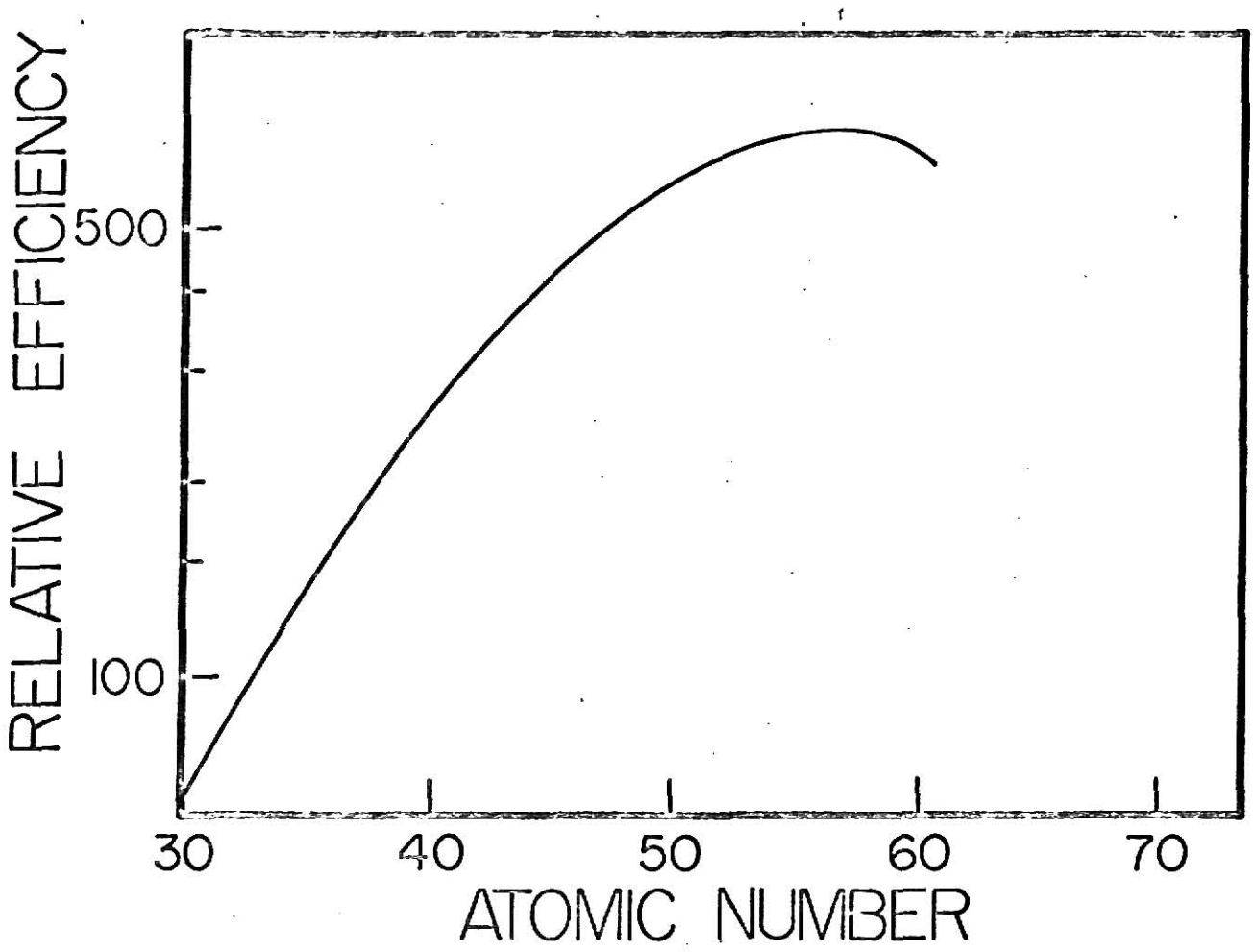


Figure 10. System Efficiency Product Curve For Am-241 As Calculated by Equation 6

Figure 11. System Efficiency Product Curve Matched To Experimental Curves For Coffee

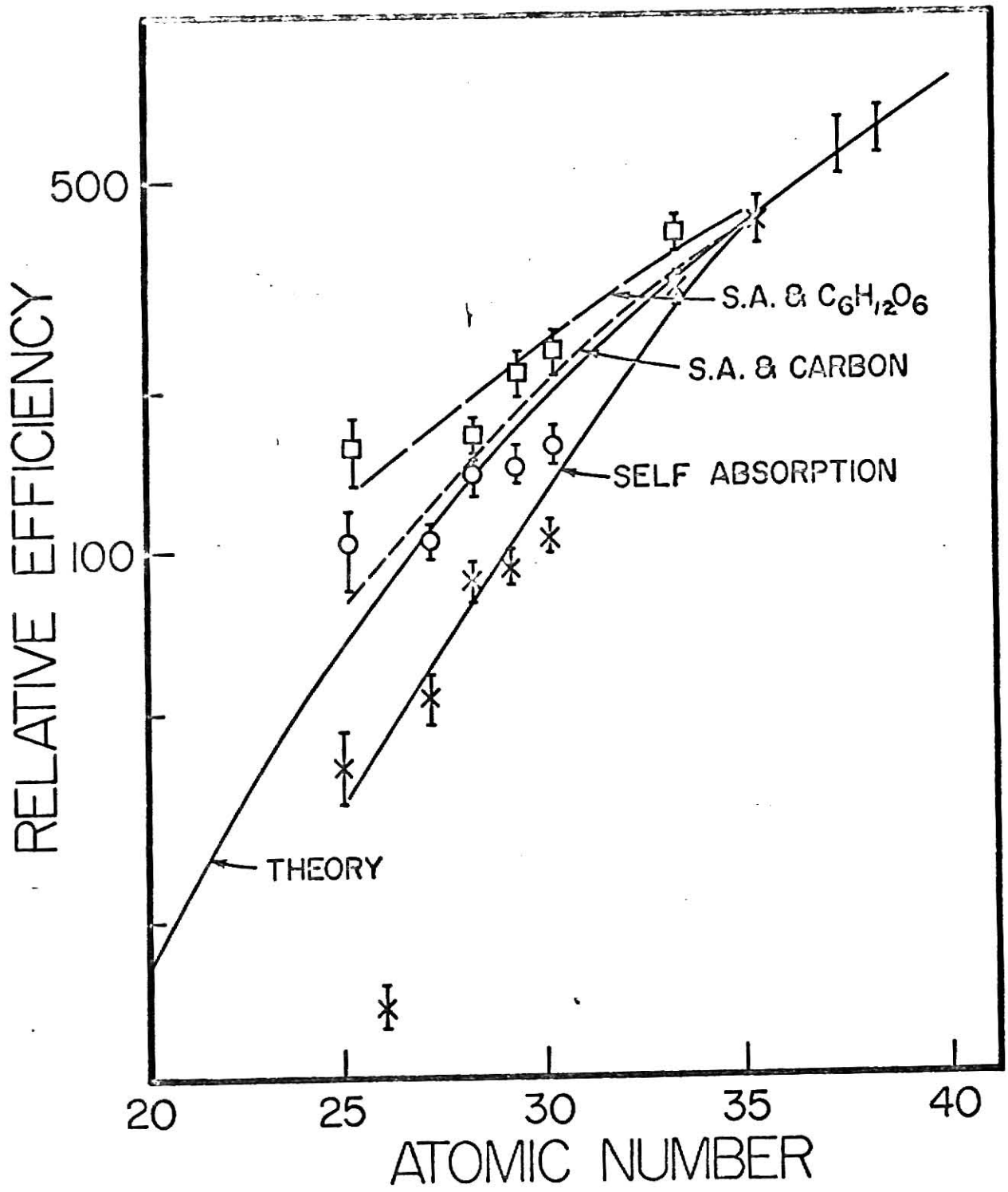

Table 1. Suggested Doping Compounds

| Atomic Number | Suggested Compound | Chemical Form | % Element Weight | Absorption Coefficient | Transmission for 0.03mm |
|---|---|---|---|---|---|
| 16 | Lithium Sulfate | $Li_2SO_4$ | 29.1 | 15.24 | 63 |
| 17 | Lithium Perchlorate | $LiClO_4$ | 33 | 16.0 | 61.8 |
| 19 | Potassium Lithium dl-Tartrate | $LiKC_4H_4O_6 \cdot H_2O$ | 18 | 2.0 | 94.2 |
| 20 | Calcium Benzoate | $Ca(C_7H_5O_2)_3 \cdot 3H_2O$ | 12 | 0.7 | 93.2 |
| 21 | Scandium Oxide | $Sc_2O_3$ | 65 | 11.1 | 71.6 |
| 22 | Titanium Dioxide | $TiO_2$ | 60 | 17.6 | 59.4 |
| 23 | Vanadium Dioxide | $VO_2$ | 61 | 17.0 | 60.0 |
| 24 | Chromium Oxalate | $CrC_2O_4 \cdot H_2O$ | 33 | 2.3 | 93.2 |
| 25 | Manganese Sulfate | $MnSO_4 \cdot H_2O$ | 32.5 | 50.0 | 86.2 |
| 26 | Potassium Ferricynate | $K_3Fe(CN)_6$ | 17 | 0.3 | 99 |
| 27 | Cobalt Sulfate | $CoSO_4 \cdot 7H_2O$ | 21 | 1.0 | 96.9 |
| 28 | Nickel Sulfate | $NiSO_4 \cdot 6H_2O$ | 22 | 1.3 | 94.8 |
| 29 | Copper Sulfate | $CuSO_4 \cdot 5H_2O$ | 25 | 1.2 | 94.6 |
| 30 | Zinc Sulfate | $ZnSO_4 \cdot 7H_2O$ | 23 | 1.1 | 94.7 |
| 31 | Gallium Acetyl Acetonate 2,4- | $Ga(C_5H_7O_2)_3$ | 19 | 0.2 | 94.2 |
| 32 | Germanium Dioxide | $GeO_2$ | 69 | 7.5 | 79.4 |
| 33 | Arsenic Trioxide | $As_2O_3$ | 75.7 | 3.7 | 88.8 |

| Atomic Number | Suggested Compound | Chemical Form | % Element Weight | Absorption Coefficient | Transmission for 0.03mm |
|---|---|---|---|---|---|
| 34 | Selenium Dioxide | $SeO_2$ | 71 | 6.0 | 83.5 |
| 35 | Calcium Bromide | $CaBr_2$ | 80.1 | 3.9 | 87.9 |
| | Calcium Bormate | $Ca(BrO_3)_2 \cdot H_2O$ | 50.1 | 2.0 | 94 |
| 37 | Rubidium Chloride | RbCl | 70.7 | 4.0 | 87.7 |
| | Rubidium Aluminum Sulfate | $RbAl(SO_4)_2 \cdot 12H_2O$ | 16 | 0.1 | 96.1 |
| 38 | Strontium Chloride | $SrCl_2 \cdot 6H_2O$ | 32.9 | 0.9 | 97.3 |
| 39 | Yttrium Nitrate | $Y(NO_3) \cdot 4H_2O$ | 26 | 0.4 | 98.8 |
| 40 | Zirconium Hydroxide | $Zr(OH)_4$ | 57 | 0.1 | 94.2 |
| 41 | Niobium Pentoxide | $Nb_2O_5$ | 35 | 1.0 | 97 |
| 42 | Sodium Molybate | $Na_2MoO_4 \cdot 2H_2O$ | 40 | 1.0 | 97 |
| 44 | Ruthenium Dioxide | $RuO_2$ | 76 | 7.2 | 97.8 |
| 45 | Rhondium Hexaamine Chloride | $Rh(NH_3)_6Cl_3$ | 33 | 0.3 | 99 |
| 46 | Palladium Flouride | $PdF_3$ | 65.5 | 3.0 | 91.4 |
| 47 | Silver Nitrate | $AgNO_3$ | 63.4 | 2.0 | 94.2 |
| 48 | Cadmium Ammonium Sulfate | $Cd(NH_4)_2(SO_4)_2 \cdot 6H_2O$ | 25.3 | 0.2 | 99 |
| 49 | Indium Methylate | $In(CH_3)_3$ | 71.8 | 0.9 | 99 |
| 50 | Tin Orthophosphate | $Sn(H_2PO_4)_2$ | 37.9 | 0.5 | 97.4 |

| Atomic Number | Suggested Compound | Chemical Form | % Element Weight | Absorption Coefficient | Transmission for 0.03mm |
|---|---|---|---|---|---|
| 51 | Antimonide Oxysulfate | $Sb_2O_2SO_4$ | 65.4 | 1.1 | 96.7 |
| 52 | Tellurium Trioxide | $TeO_3$ | 72.8 | 2.5 | 92.6 |
| 53 | Potassium Iodate | $KIO_3$ | 59.4 | 1.3 | 96.4 |
| 55 | Cesium Aluminum Sulfate | $CsAl(SO_4)_2 \cdot 12H_2O$ | 22.9 | 0.1 | 99 |
| 56 | Barium Tartrate | $BaC_4H_4O_6 \cdot H_2O$ | 45.3 | 0.5 | 98.5 |
| 57 | Lanthanum Carbonate | $La_2(CO_3)_3 \cdot 8H_2O$ | 46.2 | 0.2 | 99 |
| 58 | Cerium Sulfate | $Ce_2(SO_4)_3 \cdot 9H_2O$ | 38.3 | 0.2 | 99 |
| 59 | Praseodymium Sulfate | $Pr_2(SO_4)_2 \cdot 8H_2O$ | 40 | 0.2 | 99 |
| 60 | Neodymium Sulfate | $Nd_2(SO_4)_3 \cdot 8H_2O$ | 40 | 0.1 | 99 |

the tube. Then the tube was weighed again. The tube's contents were mixed and labeled. The disks were then prepared.

Doping was limited to a maximum of 1% of the sample weight, using a low-element-to-molecular-weight compound to minimize self-absorption by the compound. For instance, the transmission of strontium K x-rays was calculated to be 97.3% for a 1% concentration of strontium chloride. However, at 10% concentration, the transmission rate was down to 75%. If the other elements in the compound were much lighter than the critical doping element, they could be ignored since absorption would be very small. Low-level doping of the order of 100 ppm was difficult and was found to be inaccurate. Counts were usually twice the number found for high-level doping.

Multiple doping at levels of 1% concentration was not possible since the elements would absorb each other's characteristic x-rays heavily, although the effect was greater on light element x-rays than heavy element x-rays. This was seen in examining the total transmission rates of bromine and strontium in a sample, where NaBr and $SrCl_2 \cdot 6H_2O$ were both at 1% concentration. The total transmission of strontium was 91.7%, while the transmission of bromine was only 63.5%. In an ordinary sample the amount of absorption per element summed over all trace elements present was negligible if that sum of the concentrations was less than 0.2%. This doesn't include matrix

absorption. The total transmission of $K_\alpha$ x-rays per element was the product of the transmission due to each element.

C. Absorption Corrections

An experimental curve was obtained by using doped samples normalized to counts per μg of element per gm of sample per 3000 seconds after the amount of naturally occuring element in the sample in terms of counts per gram was subtracted out. The amount of element in the sample was then corrected for self-absorption using the $K_\alpha$ cross section as $P_k$. Transmission of the K line for an element was dependent upon the density, Avogadro's number, the total photoelectric cross section due to the element itself or the absorbing element, the fractional ratio of the element in its compound, the molecular weight of the compound, and the thickness of the compound. The thickness was taken as 1% of the disk thickness, 30 μm.

$$\text{Transmission} = \exp - \left(At \Sigma \frac{f p \mathcal{G}}{M}\right) \qquad (5)$$

P = density of the compound

A = Avogadro's number

$\mathcal{G}$ = total photoelectric cross section due to the element itself, or the absorbing element

M = molecular weight

f = element weight-to-molecular-weight ratio

t = thickness of the compound through which the secondary X-rays pass

The above self-absorption curve correction was adequate for light sample matrices with heavy trace elements, but the experimental curve fell short for the lighter trace elements like zinc, iron, and manganese. A more comprehensive curve correction was to consider the total absorption coefficient due to the doping element and the sample matrix. In calculating the total transmission of an element's K-line, the negative exponential of the absorption coefficient times the thickness increment was integrated over the thickness of the sample and the doping compound.

$$\text{Transmission} = \frac{1 - \exp(-Ct)}{Ct} \qquad (6)$$

$t$ = thickness of the sample in mm

$C$ = total absorption coefficient - $A_e f + A_m (1-f)$

$A_e$ = absorption of the element in the compound by the elements of the compound

$f$ = the fraction of the thickness of the matrix due to the compound

$A_m$ = absorption of the element by all the elements in the matrix other than the doping compound

In food stuffs the matrices were made up of carbon, nitrogen, oxygen, and hydrogen. Corrections were calculated for pure carbon, and glucose, a $C_6H_{12}O_6$ compound, at the disk densities. The densities listed by the CRC Chemistry and Physics handbook for carbon and glucose were two times greater than the calculated disk

densities. This is apparent in Figures 12 and 13. In general, light element matrix effects were extremely important for elements with K -lines below 10 Kev, and negligible for K -lines above 16 Kev. To correct for the effects of matrix and doping compounds, the calculated transmission in each case was divided into the total number of counts in the normalized peak area into terms of counts per mg of element per gram of sample per 3000 seconds. The heaviest element point in the matrix was fixed to the theory curve as in the self-absorption case. Then, the experimental and theory curves were compared.

D. Effects of Density and Composition of Samples

The experimental curves deviated from the theory curve depending on their makeup and density. The greater the density and the heavier the elemental makeup, the lower the doped levels per element were. Coffee, milk, and orchard leaves were approximately the same weight per disk, but the doping levels varied. The doping levels were 157 $\pm$ 10, 125 $\pm$ 6, and 146 $\pm$ 16 counts/$\mu$g of strontium / gm of sample/3000 seconds respectively. The coffee contained lighter elements than the orchard leaves and the milk, hence it had the highest number of counts per microgram of strontium. Orchard leaves contained a high proportion of heavy elements in addition to the carbon. Thus, it was intermediate between the

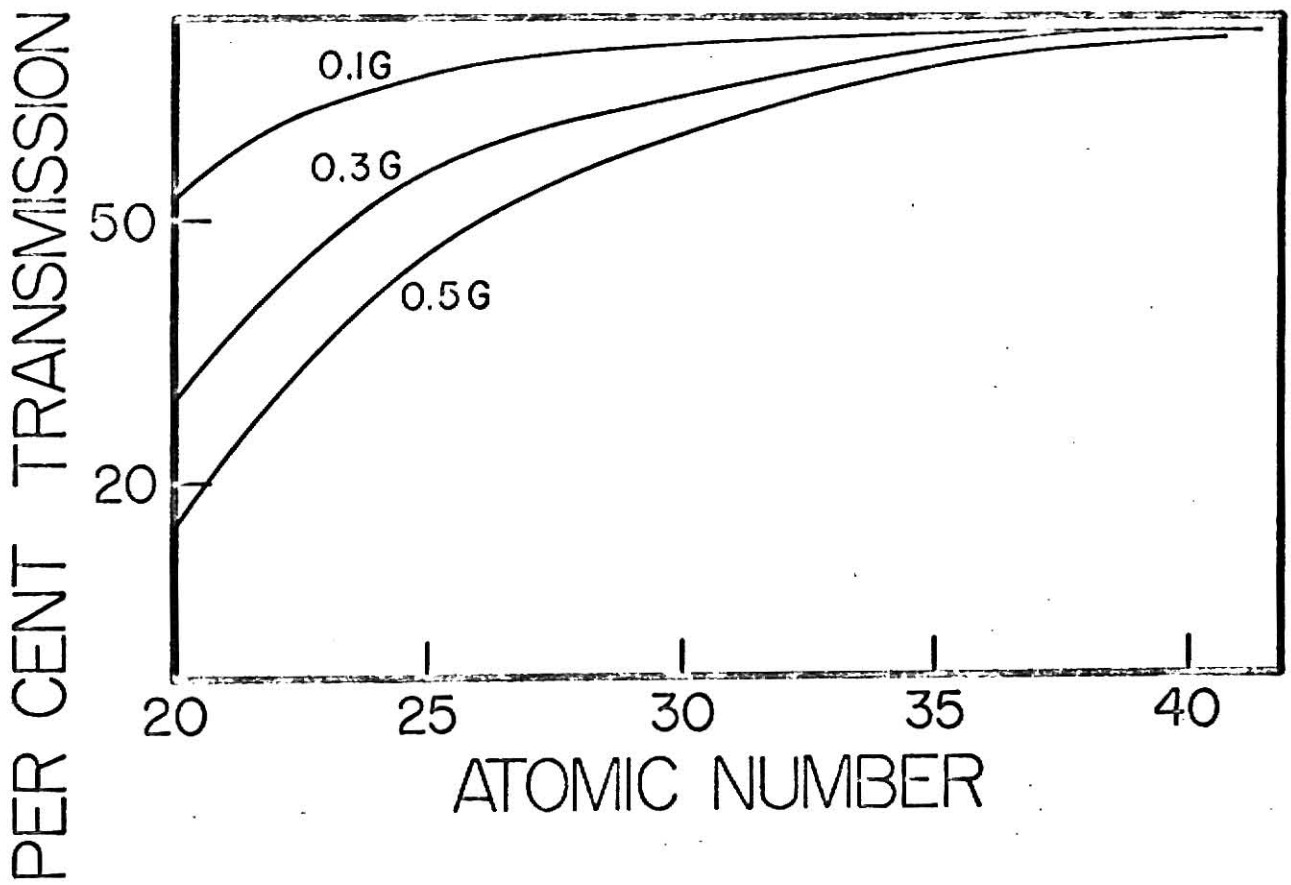


Figure 12. Percent Transmission of Elements, Z= 20 to 45, $K_\alpha$ X-rays Through a Low-Doped 3mm Carbon Matrix Based on the Weight per Disk

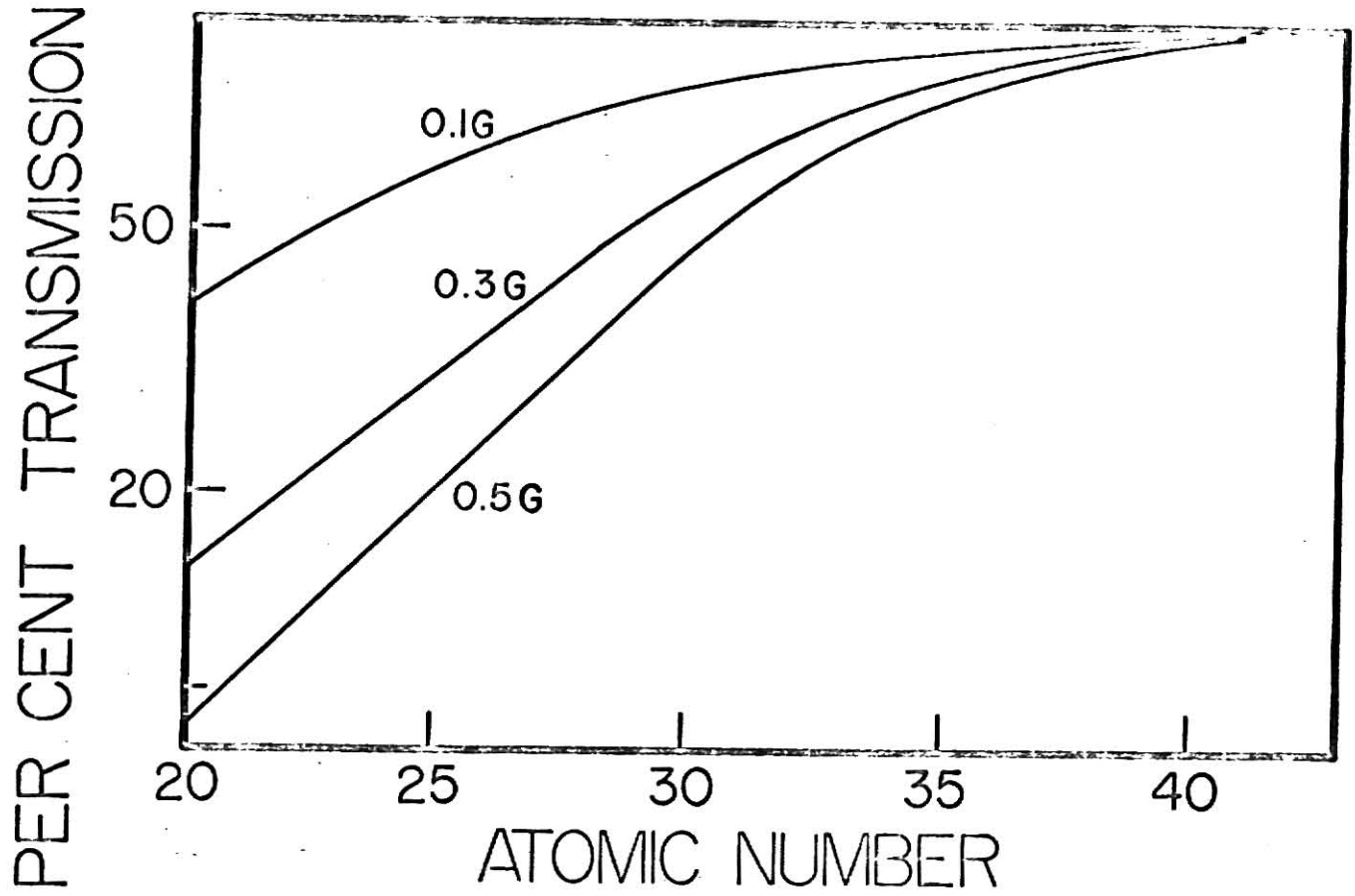


Figure 13. Percent Transmission of Elements, Z= 20 to 40, $K_{\alpha}$ X-rays Through A Low-Doped 3mm Glucose Matrix Based on the Weight per Disk

coffee and the milk. Milk contained a high amount of carbohydrates which had a photoelectric cross section 2.26 times greater than that of carbon. Therefore, it absored more strontium K x-rays than the coffee or the leaves. This effect was observable between the strontium containing rocks and Koolaid, and between the turkey ash and tea as well. Because the exact composition of all these items is unknown, it was difficult to compare the observed values to the calculated values for a carbon or a glucose matrix as in Tables 2 through 9.

Density effects were observable in a comparison of the strontium levels in tea, milk, and Koolaid. These levels were $157 \pm 10$, $125 \pm 6$, and $72 \pm 11$ counts/$\mu$g/gm/3000 seconds, respectively. The weights per sample were .10gm, .30gm, and .60gm respectively. Although the matrix compositions of these items were different, it was apparent that the increasing density decreased the counts/$\mu$g/gm/3000 seconds. The calculated per cent transmission decreased as the density increased for a pure carbon or a glucose matrix. The decrease in per cent transmission from tea to Koolaid was 100%, 80%, and 45%. In contrast, the decrease in per cent transmission for carbon at similar densities was 100%, 91%, and 79%; for glucose at similar densities, it was 100%, 83%, and 63%.

To determine the amount of the given element in the sample,

1% Doping Levels In Samples

Table 2. Coffee (250-300mg/disk)

| Atomic Number | S.A. Corrected Cts/ugof Z/gm | Theory Product | Trans % D.C. | S.A. Fit | Matrix Corrected Carbon | $C_6H_{12}O_6$ |
|---|---|---|---|---|---|---|
| 38 | 157 ± 10 | 629 | 98 | 630 ± 50 | 630 | 630 |
| 37 | 150 ± 15 | 559 | 86 | 600 ± 70 | 570 | 630 |
| 35 | 106 ± 4 | 437 | 86 | 425 ± 30 | 400 | 420 |
| 33 | 80.5 ± 5.2 | 334 | 92 | 320 ± 20 | 340 | 410 |
| 30 | 26.7 ± 1.0 | 206 | 97 | 107 ± 6 | 153 | 235 |
| 29 | 23.4 ± 1.9 | 166 | 96 | 94 ± 9 | 145 | 222 |
| 28 | 21.8 ± 2.2 | 136 | 92 | 88 ± 9 | 136 | 232 |
| 27 | 13.4 ± 2.6 | 109 | 95 | 52 ± 6 | 101 | 152 |
| 26 | 3.4 ± 2.0 | 86 | 99 | 13.7±10 | 77 | 125 |
| 25 | 9.7 ± 1.6 | 68 | 86 | 39 ± 8 | 105 | 163 |

The iron cts/µg/gm estimate was based on the self-absorption corrected curve. 12.1 ± 1.0 cts/µg of iron/gm

Table 3. Tea (100mg/disk)

| Atomic Number | S.A. Corrected Cts/ug of Z/gm | Theory Product | Trans % D.C. | S.A. Fit | Matrix Corrected Carbon | $C_6H_{12}O_6$ |
|---|---|---|---|---|---|---|
| 37 | 148 ± 1 | 560 | 82 | 560± 4 | ** | ** |
| 30 | 63 ± 4 | 210 | 94 | 240 ± 30 | ** | ** |

The bromine cts/µg/gm estimate was based on the self-absorption corrected curve. 115 ± 1 cts/µg of bromine/gm

The manganese cts/ug/gm estimate was based on the self-absorption corrected curve. 18± 1 cts/µg of manganese/gm

Table 4. Milk (200-300mg/disk)

| Atomic Number | S.A. Corrected Cts/ug of Z/gm | Theory Product | Trans % D.C. | S.A. Fit | Matrix Corrected Carbon | $C_6H_{12}C_6$ |
|---|---|---|---|---|---|---|
| 38 | 125 ± 6 | 629 | 97 | 630 ± 40 | 630 | 630 |
| 37 | 93 ± 10 | 559 | 86 | 500 ± 130 | 480 | 520 |
| 35 | 93 ± 14 | 437 | 93 | 460 ± 60 | 470 | 490 |
| 33 | 46 ± 4 | 334 | 86 | 230 ± 30 | 230 | 290 |
| 30 | 45 ± 9 | 206 | 96 | 210 ± 50 | 290 | 430 |
| 29 | 28 ± 2 | 166 | 97 | 139 ± 20 | 210 | 550 |
| 26 | 19 ± 3 | 86 | 99 | 97 ± 10 | 227 | 396 |

Table 5. Orchard Leaves (250-300mg/disk)

| Atomic Number | S.A. Corrected Cts/µg of Z/gm | Theory Product | Trans % D.C. | S.A. Fit | Matrix Corrected Carbon | $C_6H_{12}C_6$ |
|---|---|---|---|---|---|---|
| 38 | 146 ± 16 | 629 | 96 | 630 ± 50 | 630 | 630 |
| 37 | 155 ± 11 | 556 | 81 | 630 ± 70 | 550 | 580 |
| 33 | 120 ± 11 | 334 | 71 | 490 ± 60 | 366 | 450 |
| 30 | 58 ± 1 | 206 | 97 | 210 ± 1 | 276 | 420 |
| 29 | 35 ± 7 | 166 | 96 | 104 ± 20 | 162 | 358 |
| 25 | 12 ± 1 | 68 | 62 | 45 ± 3 | 95 | 138 |

The Koolaid doped level for strontium was 71.9 ± 11 cts/ug/g. There was approximately 300mg of Koolaid per disk.

Table 6. Turkey Ash (100mg/disk)

| Atomic Number | S.A. Corrected Cts/ug of Z/gm | Theory Product | Trans % D.C. | S.A. Fit | Matrix Corrected Carbon | $C_6H_{12}O_6$ |
|---|---|---|---|---|---|---|
| 37 | 109 ± 27 | 556 | 83 | 560 ± 130 | 560 | 560 |
| 33 | 81 ± 1 | 334 | 89 | 350 ± 2 | 340 | 370 |
| 30 | 32 ± 1 | 206 | 98 | 164 ± 3 | 161 | 195 |
| 29 | 26 ± 1 | 166 | 97 | 145 ± 2 | 147 | 195 |
| 26 | 10 ± 1 | 86 | 99 | 4.3± 0.4 | 64 | 89 |
| 25 | 12 ± 1 | 68 | 65 | 7.2± 1 | 79 | 105 |

Table 7. Doping Levels of Bromine in Flour (350mg/disk)

| Flour | Time: 3000seconds | Number of Samples: 3 |
|---|---|---|
| ppm | counts/µg of Br/gm | Ratio with 669 ppm |
| 669 | 128 ± 17 | 1 |
| 444 | 132 ± 14 | 1 |
| 199 | 129 ± 42 | 1 |
| 42 | 283 ± 76 | 2.21 |
| 12 | 261 ± 95 | 2.04 |

Table 8. Doping Levels in Rocks

| Powdered | Time: 3000seconds | | Number of Samples: 2 | |
|---|---|---|---|---|
| Type | Rubidium ppm | Counts/µg of Rb | Strontium ppm | Counts/µg |
| AGV-1 | 89.4 | 32.0± 2.8 | 657 | 64.4±5.3 |
| G-2 | 234 | 42.6± 2.0 | 463 | 81.0±4.4 |

the peak area due to the naturally occurring element in the sample was subtracted from the total peak area for the dope sample. The remaining peak area is due to the doping element alone, and can be put in terms of counts/ μg of element/ gm of sample/ 3000 seconds. By dividing the ordinary sample's peak area for that element (counts/ gm of sample/ 3000 seconds) with the doped peak area, the amount of that trace element in a sample is known in terms of μg of element/ gm of sample or in parts per million (ppm).

There is a technical problem for the lighter elements because of the overlapping of the $K_\alpha$ and the $K_\beta$ x-rays. These peaks in a sample could not be separated physically, so the $K_\alpha$ was taken to be a fraction of the sum of both peaks. This problem was especially complicated for the potassium and calcium peaks since the $K_\beta$ of potassium overlapped the $K_\alpha$ peak of calcium.

The iron doping levels for coffee, milk, and ash were inconsistent with the other experimental points established for each material. The points were usually one-third of the value estimated for iron using the self-absorption corrected curve, although the experimental values varied greatly about this one-third ratio. This may be due to the tendency of potassium ferricynate to clump and stick in powder form.

Element self-absorption was minimized in doped samples, and was no problem in most ordinary samples, Matrix effects became extremely important for elements with atomic numbers below that of nickel. From strontium to arsenic the theory curve matched well with the corrected self-absorption and matrix experimental curves. Below arsenic, the self-absorption curve fell below the theory curve depending upon the density and makeup of the matrix. The compound and matrix absorption curves appeared to overcorrect the experimental curves below nickel. In these cases corrections were made for both a pure carbon matrix and a glucose matrix at the densities used.

## E. Error Analysis

Individual sample error in peak area determination was less than 10% based on the baseline fit to the background. The deviation per element from a five-sample averaged value ranged from 5% to 15%. The individual doping error was less than 1%, but the average deviation from the doping level values, averaged over two different concentrations with three doped samples per concentration, was approximately 10%. The total error is the square root of the sum of the squares of the individual errors. This total error was a maximum of 22%.

The statistical uncertainty for N counts is the square root of N. The per cent deviation was the reciprocal of the square root of N. The net deviation was the square root of the sum of the peak counts and the background counts. The per cent deviation of the total counts equal to 100 times the net deviation divided by the peak counts. The minimum detectable count for peak detection was taken to be $2\sqrt{N_b}$. For instance, if the background count under a 10 channel peak was 500 counts/channel, 46 counts per channel or 460 counts per 10 channel peak would be necessary for detection. At the strontium $K_\alpha$ peak this meant that the minimum detectable limit was approximately 5 ppm. The minimum detectable limit for the manganese $K_\alpha$ peak was 40 ppm using the same criterion. The minimum detectable limit per element decreased as the number of counts/ug of element increased. Therefore, the minimum detectable limit per element was dependent on the sample density and makeup. For a given matrix the minimum detectable limit increased as the atomic number of the element decreased.

# CHAPTER FIVE

## RESULTS AND DISCUSSION

Powdered beverages such as coffee, milk, tea, and flavoraid are part of the diet of test animals as well as man. The major components of these drinks are the lighter elements in addition to a nonquantifiable amount of potassium and calcium. The toxicity levels considered in this paper are those for a 70 Kg man eating a dry weight of 750 gm per day. For most elements these toxicity levels are in ppms.

Instant coffees included iron, bromine, rubidium, and strontium as seen on Table 9. They may have contained copper and zinc in amounts less than 16 ppm. None of the trace elements present were in toxic amounts. Although the amount of rubidium in instant coffees was rather high in comparison to some foods, it was not outside the normal range of rubidium in foods which is 1-200 ppm. The amounts of bromine and rubidium appeared to vary between brands. The iron content was based on the self-absorption curve estimate rather than the value calculated from doped samples. The doped level of iron was one-third the expected value. Regular coffees also contained copper in detectable quantities, but some of these regular grinds lacked bromine. The average weight per sample for all coffees ranged from .2gm to .3gm.

Results of Sample Analysis
in ppm

Running Time: 3000 seconds

Table 9. Coffee

Instants — Number of Samples: 5

| Brand Product | Iron | Bromine | Rubidium | Strontium |
|---|---|---|---|---|
| Brim | 119± 51 | 28.2± 19 | 169± 80 | 25.7± 8.5 |
| Sanka | 94± 52 | 18.8± 47 | 131± 67 | 18.3± 6.6 |
| Maxwell House | 101± 65 | 30.4± 11 | 123± 20 | 19.3± 6.0 |
| Folgers | 115± 48 | 23.3± 22 | 165± 24 | 17.2± 6.3 |

Instants — Number of Samples: 1

| Brand Product | Iron | Bromine | Rubidium | Strontium |
|---|---|---|---|---|
| Airway | 177± 26 | ** | 215± 12 | 19 ± 2.4 |
| Taster's Choice | 125±26 | 60.5± 4 | 144± 12 | 25.4± 2.5 |
| Maxim | 49± 36 | ** | 251± 12 | 48 ± 3.3 |

Regular Grinds — Number of Samples: 1

| Brand Product | Iron | Copper | Rubidium | Strontium |
|---|---|---|---|---|
| Folgers | 75± 25 | 52± 12 | 75± 37 | 14.3± 1.8 |
| Edwards | 193± 41 | 100± 21 | 133± 6 | 16.4± 3.1 |
| Butternut | 140± 30 | 81± 15 | 102± 5 | 11.9± 2.2 |
| Maxwell House | 131± 30 | 89± 14 | 100± 4 | 13.3± 2.0 |

Maxwell House contains 40± 13 ppm of bromine.

Table 10. Tea

Instants — Number of Samples: 5

| Brand Product | Manganese | Zinc | Bromine | Rubidium |
|---|---|---|---|---|
| Nestea | 640± 303 | 40± 65 | 15.8± 18 | 405± 170 |

Results of Sample Analysis
in ppm

Running Time: 3000 seconds

Table 11. Powdered Milk

| Brand Product And Number of Samples | Copper | Zinc | Bromine | Rubidium | Strontium |
|---|---|---|---|---|---|
| Carnation-- 5 | 13± 40 | 73± 42 | 60± 72 | 51± 47 | 11.1± 7.3 |
| Food Club-- 1 | ** | 63± 10 | 56± 5 | 53± 5 | 6.6± 3.9 |

Table 12. Flavorades

Powdered — Number of Samples: 5

| Brand Product | Flavor | Strontium | Calcium |
|---|---|---|---|
| Koolaid | Grape | 55.9± 19.3 | Listed - 4% |
| | Orange | 59.6± 39.4 | |
| | Cherry (I) | 55.4± 29.7 | |
| | Cherry (II) | ** | * * |
| Flavorade | All Flavors | ** | * * |

Table 13. Turkey Ash Number of Samples: 2

| Iron | Zinc | Rubidium |
|---|---|---|
| 640± 190 | 1,570± 80 | 1,280± 60 |

Table 14. Powdered Orchard Leaves Number of Samples: 2

| Value | Manganese | Copper | Zinc | Arsenic | Rubidium | Strontiu |
|---|---|---|---|---|---|---|
| Listed | 91± 4 | 12± 1 | 25±3 | 14± 2 | 12 ± 1 | 37 |
| Calculated | 81± 25 | 39± 14 | 26±3 | 43± 3 | 23 ± 3 | 67± 8 |

Carnation instant milk included copper, zinc, bromine, rubidium, and strontium, as seen in Table 11. None of the trace elements were in toxic amounts. Each element was highly variable per sample, especially copper. The matrix was different from coffee although the weight per disk was the same. The different standard counts/µg of element/gm of sample/3000 seconds from the milk doping system were probably due to the very high carbohydrate concentrations in the milk samples. The Food Club instant milk sample varied from the Carnation samples as indicated in Table 11. The Food Club sample contained no copper and only a lesser amount of strontium. Such results were based only on one sample, however.

Nestea instant tea included manganese, zinc, bromine, and rubidium, as shown in Table 10. None of the trace elements are in toxic amounts, although the manganese content was extremely high. The rubidium content was also high. The amount of elements in the samples varied. Doping and mixing in a tea matrix was extremely difficult due to the light density of tea. The weight per sample was .10gm. Therefore, the doping levels were fixed using the zinc and the rubidium standardized values. Manganese and bromine levels were estimated using the resulting curve. Since the tea was lighter than coffee, the doping levels were higher.

Koolaid included calcium and strontium as indicated in Table 12. Neither of these elements was present in dangerous amounts. There was no significant variation between flavors with the exception of the newer type of cherry flavor. The newer cherry flavor did not contain strontium. The strontium in Koolaid was approximately 50 ppm. This was not listed on the packages. The weight per sample was .60gm, and the doping level value for strontium was about one-half that of coffee. This is due to the density difference and the differing makeup of coffee and Koolaid. Ordinary flavorades contain no trace elements.

Orchard leaves, listed in Table 14, powder was useful in checking the system's accuracy, although the recommended drying procedure caused some problems.[25] The standardized doping levels fixed for strontium followed the theory curve reasonably well when corrected for self-absorption of the element and the matrix. The calculated amounts of rubidium and strontium were two times greater than the listed amounts, while the copper and arsenic contents were three times greater. This could have been due to the heavy element L x-rays which raised the background in the neighboring area for the nondoped samples. The matrix properties appeared to be intermediate between that of coffee and milk, as were the doping levels.

If the standard tables for orchard leaves were correct, an estimate of the number of counts/μg/gm/3000 seconds could be made for each element listed using the nondoped samples alone. However, these levels could not be correlated to the calculated efficiency curve. These levels followed no general pattern due to a low peak-to-background ratio. This problem is paralleled by the low level doping and mixing problem for bromine in flour as seen in Table 7. The counts/μg/gm/3000 seconds were the same for doping levels between 600 ppm to 200 ppm, but below 100 ppm the counts/μg/gm/3000 seconds doubled. The error margin also increased seven times. Here again, this problem may have been due to the background fit.

Elements such as lead are considered "dangerous" at 3 ppm.[22] But as we have seen in the first half of this chapter, the Cd-109 source has a low detectable limit of 6 ppm for K x-rays with energies similar to the L x-rays of lead. Mercury in the average human head hair is approximately 8.8 ppm. In dental assistants' head hair, mercury is rated at 32 ppm. A toxic level would be seven times the normal amount in head hair.[23] This toxic level of mercury should be marginally detectable using its characteristic L x-rays. The toxic level of arsenic, 6.7 - 66.6 ppm, is marginally detectable using arsenic's K line. Both copper and antimony toxic levels, several

100 ppm, are readily detectable using their K-lines.[22] Other elements like rubidium have an estimated toxic level of 12,000 ppm.[24] The toxic levels for such elements are easily detectable.

None of the foods examined contained toxic amounts of trace elements as far as could be detected. The rubidium content in the coffee was on the high side of the range of rubidium in foods, 200ppm. There were qualitative differences between the regular grind coffees and the instant coffees. Copper appeared in the regular grind spectra, but was lacking in the instant's. It should be possible to use this technique to determine at which production stage the copper is lost from the coffee. This technique's effectiveness is maximized for high atomic number elements in light and medium density foods. Thus, many food stuffs can be screened by this technique to determine qualitatively and quantitatively the trace elements in foods that need to be indexed in food catalogues or screened for toxic elements.

# BIBLIOGRAPHY


1. Seaman, G.G., and Shane, K. C. "Trace Element Analysis by X-ray Fluorescence with an External Proton Bean," Nuc. Instr. 126 (1975) 473-74.

2. Martin, Richard, "Proton-induced X-ray Fluorescence Analysis of Trace Elements in Wheat Flour, Kansas State University, 1973 (unpublished Master's Thesis).

3. Volchmann, Monty, "Analysis of Surface Contaminants in Biological Samples by Characteristic X-ray Analysis," Kansas State University, 1972 (unpublished Master's Thesis, 1972).

4. Woldseth, R., X-ray Energy Spectrometry, Kervex Corp. pp 3.15 - 3.19.

5. Ibid., Woldseth, R.C., pp 2.38 - 2.60.

6. Cothern, C. R., Mansel, H. L., and Millette, J. R., "Determination of the Overall Efficiency in X-ray Fluorescence for the Situation where the Exciting Source Produces a Wide Range of Energies," University of Dayton. (to be published).

7. Op. Cit., Woldseth, pp 1.11 - 1.16.

8. Op. Cit., Woldseth, pp 1.09 - 1.10.

9. Scofield, James, "Theoretical Photo Ionization Cross Sections from 1 to 1500 Kev., Lawrence Livermore Lab, 1973.

10. Cooper, J. A., "Comparison of Particle and Photon Excited X-ray Fluorescence Applied to Trace Element Measurements of Environmental Samples," Nuclear Instr. & Methods 106:525+, (1973).

11. Op. Cit., Woldseth, pp 2.38 -2.47.

12. Ortec 7000 Series Si (Li) X-ray Detector Operating and Service Manual, 1970.

13. Ibid., Ortec p. 10.

14. Op. Cit., Woldseth, R. C., p. 2.41.

15. Op. Cit., Woldseth, R. C., p. 2.15.

16. Op. Cit., Woldseth, R. C. pp. 2.1 +.

17. Op. Cit., Ortec pp. 8 - 9.

18. Op. Cit., Woldseth, R. C. p. 2.29.

19. Op. Cit., Woldseth, R. C., pp. 2.1+.

20. Op. Cit., Cothern, C. R. pp. 3-4.

21. Op. Cit., pp. 3.1+.

22. Bowen, H., Trace Elements in Biochemistry Academic Press, 1966, pp. 116-7.

23. Underwood, E. J., Trace Elements in Human and Animal Nutrition, Academic Press, 1971, pp. 443-6.

24. Ibid., Underwood, E. J., pp. 446-7.

25. National Bureau of Standards Certificate of Analysis SRM:1571, Orchard Leaves, Washington, D. C., 1971.

## ACKNOWLEDGEMENT

The author would like to thank Dr. G. G. Seaman for his suggestions, assistance, and encouragement during this project; the Agricultural Experiment Station for their financial assistance; my aunt Lena Hatt for her help, and my family for their moral support.

# TRACE ELEMENT ANALYSIS OF POWDERED BEVERAGES AND OTHER MATERIALS BY X-RAY FLOURESCENCE

by

CHERYL K. DELLAI

B. S., University of Wyoming, 1974

---

AN ABSTRACT OF A MASTER'S THESIS

submitted in partial fulfillment of the

requirements for the degree

MASTER OF SCIENCE

Department of Physics

KANSAS STATE UNIVERSITY
Manhattan, Kansas

1976

## ABSTRACT

Using x-ray stimulated x-ray fluorescence, various powdered beverages were analyzed for trace elements. With the exception of manganese in tea, all trace elements were than 300 ppm each in the beverage samples. The minimum detectable limit was found to vary with the element and was generally in the 10 ppm. Rubidium, strontium, and calcium were the most common elements in these powdered beverages. This technique of x-ray fluorescence has proven to be a useful method for trace element analysis.